A high-resolution solid-state NMR study on nano-structured HZSM-5 zeolite

Weiping Zhang [a], Xinhe Bao [a,*], Xinwen Guo [b] and Xiangsheng Wang [b]

[a] *State Key Laboratory of Catalysis, Dalian Institute of Chemical Physics, Chinese Academy of Sciences, Dalian 116023, PR China*
E-mail: xhbao@gingko.dlut.edu.cn

[b] *Laboratory of Comprehensive Utilization of Carbonaceous Resources, Dalian University of Technology, Dalian 116012, PR China*

Received 7 December 1998; accepted 26 March 1999

Variations in the structure and acidity properties of HZSM-5 zeolites with reduction in crystal sizes down to nanoscale (less than 100 nm) have been investigated by XRD, TEM and solid-state NMR with a system capable of *in situ* sample pretreatment. As evidenced by a combination of ^{27}Al MAS NMR, ^{29}Si MAS, CP/MAS NMR and ^{1}H MAS NMR techniques, the downsize of the zeolite crystal leads to an obvious line broadening of the ^{27}Al, ^{29}Si MAS NMR spectrum, an increasing of the silanol concentration on the external surface, and a pronounced alteration of the acidity distribution between the external and internal surfaces of the zeolite. In a HZSM-5 zeolite with an average size at about 70 nm, the nonacidic hydroxyl groups (silanols) are about 14% with respect to the total amount of Si, while only 4% of such hydroxyl groups exist in the same kind of zeolite at 1000 nm crystal size. The result of ^{1}H MAS NMR obtained using Fluorinert® FC-43 (perfluorotributyl amine) as a probe molecule demonstrates that most of the silanols are located on the external surface of the zeolite. Moreover, the concentration of Brønsted acid sites on the external surface of the nano-structured zeolite appears to be distinctly higher than that of the microsized zeolite.

Keywords: solid-state NMR, nano-structured HZSM-5 zeolite, probe molecule, perfluorotributyl amine ($(n$-$C_4F_9)_3N$)

1. Introduction

Ultrafine zeolites as a new member of nano-structured particles have attracted considerable interest in the field of catalysis in recent years. It is generally recognized that particle sizes of zeolites have a significant influence on the catalytic performance, particularly in reactions involving the external surface and controlled by a diffusion process [1,2]. As demonstrated, in catalytic cracking of vacuum gas oil using Y zeolite as the catalyst, smaller crystal sizes produced more gasoline and diesel, but less coke and gases [3,4]. An aggregated HZSM-5 zeolite consisting of small crystallites showed long catalytic life and high selectivities for C_5 hydrocarbon and aromatics in the conversion of methanol to hydrocarbons [5]. These unique effects are usually ascribed to alternations of apparent properties with the particle sizes, that is, the increase of the external surface and the shortening of the active channels of the zeolites. To date, extensive investigations concerning structure and acidity, as well as the catalytic characteristics, have been carried out with various zeolites [6–8]. However, the variation of structure and acidity as a function of the zeolite crystal size, in particular when the crystal size is down to nanoscale, has not been well investigated due partially to the difficulties in obtaining the zeolite at desired dimensions, and also to the lacking of sensitive methods for characterization. In the present study, ZSM-5 zeolites with various crystal sizes down to 70 nm have been synthesized by controlling the amount of alkali metal salt in the common hydrothermal process. A solid-state MAS NMR with a device available for *in situ* sample pretreatment, including vacuum dehydration, selective adsorption and catalytic reaction, has been employed, and variations of structure and acidity properties of the obtained HZSM-5 zeolites have been characterized. By assisting with the selective adsorption of Fluorinert® FC-43 (perfluorotributyl amine ($(n$-$C_4F_9)_3N$), the position of silanols and the Brønsted acidity distribution between the external and internal surfaces of the various zeolites have been identified.

2. Experimental

2.1. Sample preparation and characterization

ZSM-5 zeolite samples were synthesized by well-known hydrothermal techniques using n-butylamine as the template. Commercial water glass, aluminium sulfate and sodium hydroxide were used as starting materials. The crystal dimension of the zeolites was controlled by changing the duration and temperature of crystallization as well as the amount of alkali metal salt such as NaCl [9]. The filter obtained was washed by deionized water and dried at 393 K for 2 h. The as-prepared zeolite was calcined at 923 K in air for 5 h to remove the organic template, and then converted to the proton form by repeated ion exchange with 1.0 N HCl.

The structure of the obtained zeolites has been checked by a D/max-γb type X-ray diffractometer (Rigaku) using monochromatic Cu Kα radiation (40 kV and 100 mA), and

* To whom correspondence should be addressed.

the relative crystallinity of HZSM-5 was calculated based on the intensity of the peaks of angle $2\theta = 22$–25° in the XRD pattern [5]. The dimension and morphology of the synthesized samples were observed using a transmission electron microscope (TEM Hitachi H-600) at magnification between 5,000 and 100,000.

2.2. NMR measurements

It is extremely difficult to perform an on-flow MAS NMR experiment due to the requirement of a high spinning rate of the sample rotor for obtaining a solid-state NMR spectrum with reasonable resolution. In order to recreate catalytic reaction conditions in an environment suitable for NMR spectroscopy, a special device for on-line treatment of zeolite samples has been designed and manufactured. It is functionally analogous to the CAVERN apparatus developed by Haw and co-workers [10–12]. By this system, the solid sample can be heated up to about 1000 K in vacuum for dehydration and exposed to several different gases parallelly or separately, depending on the requirements for adsorption and reaction. After the treatment, the sample can be filled *in situ* into a NMR rotor, sealed and transferred to the spectrometer without exposure to air. In the present experiment, the zeolites were dehydrated typically at 673 K and a base pressure below 10^{-2} Pa for 10–20 h. The selective adsorption using Fluorinert® FC-43 (from Acros Organics) was performed by exposing the dehydrated sample to its saturated vapor pressure at room temperature for 30 min and then evacuated for a while to remove the physical adsorbates on the surface.

All NMR spectra were accumulated at room temperature on a Bruker DRX-400 spectrometer with BBO MAS probehead using 4 mm ZrO_2 rotors. ^{29}Si MAS NMR spectra with high-power proton decoupling were recorded at 79.5 MHz using a 0.8 μs $\pi/8$ pulse with a 4 s repetition time and 2,000 scans. $^{1}H \rightarrow {}^{29}Si$ CP/MAS NMR experiments were performed with a 4 s repetition time, 4,000 scans and contact time of 1.5 ms. All ^{29}Si spectra were recorded on samples spun at 4 kHz and referenced to DSS. ^{27}Al MAS NMR spectra were recorded with high-power proton decoupling at 104.3 MHz using 0.75 μs $\pi/12$ pulse with a 3 s repetition time and 500 scans. ^{1}H MAS NMR spectra were collected at 400.1 MHz using single-pulse experiments with 1 μs $\pi/10$ pulse and a 4 s repetition time and 200 scans. All ^{27}Al and ^{1}H MAS NMR spectra were recorded with samples spun at 8 kHz, and chemical shifts were referenced to 1% aqueous $Al(H_2O)_6^{3+}$ and saturated aqueous solution of DSS, respectively.

3. Results and discussion

3.1. Structure of the zeolites

Figure 1 shows the TEM images from the samples synthesized with and without addition of NaCl in the precursor

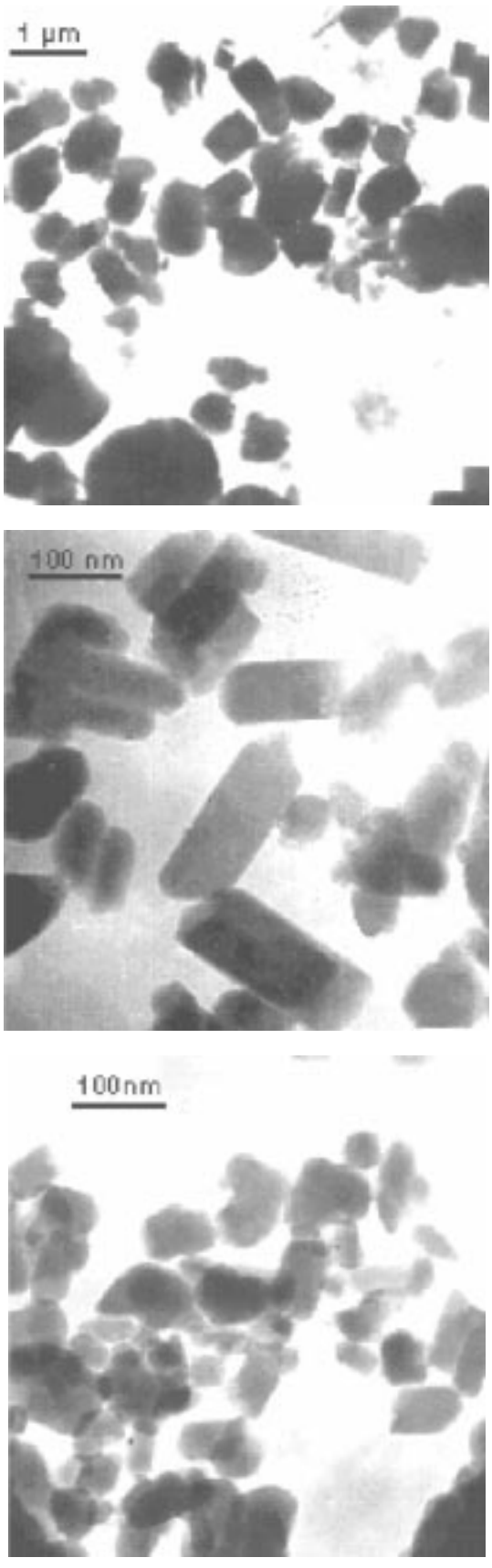

Figure 1. TEM images from samples synthesized without NaCl (a), with smaller amount of NaCl (b) and with larger amount of NaCl (c) in the precursor for crystallization.

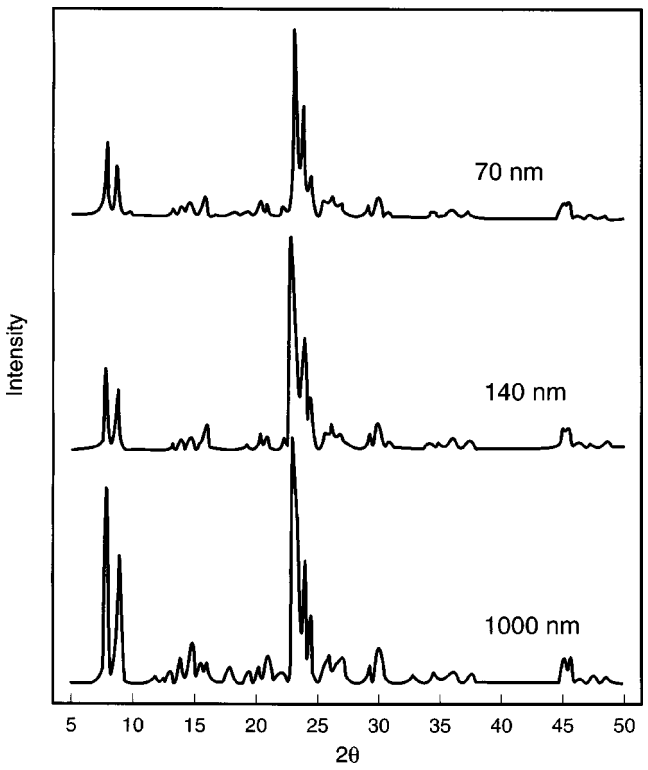

Figure 2. XRD patterns from samples with different crystal sizes.

mixture for crystallization. The addition of NaCl led to a decrease in crystal size of the resultant sample. As presented, the crystal sizes at a maximum distribution of the particle are about 140 (image (b)) and 70 nm (image (c)) when the amount of NaCl in the precursor mixture for crystallization is increased, while the average size of the sample obtained under the same condition without the addition of NaCl is about 1000 nm (image (a)). The crystals with microsizes show a rectangular shape (image (a)), while the nano-structured particles exhibit typical aggregated elliptic shapes (image (c)), which are due tentatively to the strong surface free energy of the small particles [13]. The corresponding X-ray diffraction patterns are shown in figure 2. As evidenced, all the samples exhibit the typical ZSM-5 structural characteristics (MFI). The apparent crystallinity shows to lower with the decrease of the crystal size, as listed in table 1, which is ascribed to the occurrence of extinction effects caused by the coexistence of the particles with smaller sizes in the samples [14].

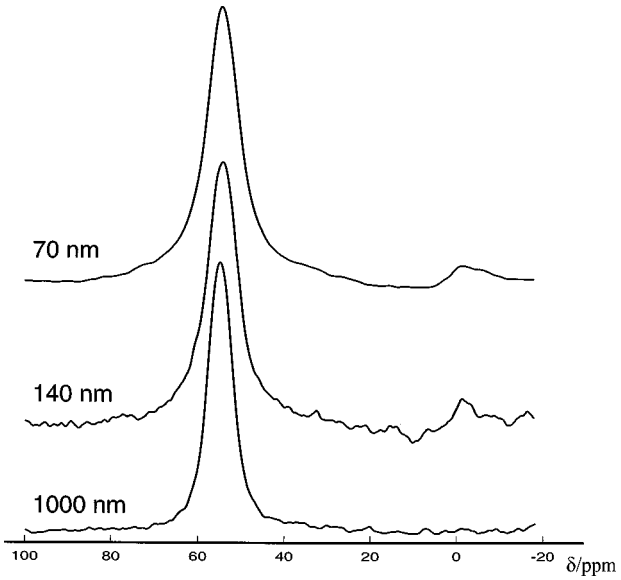

Figure 3. ^{27}Al MAS NMR spectra of HZSM-5 zeolites with different crystal sizes. The 56 ppm signal stems from four-coordinated framework Al and the 0 ppm signal is due to six-coordinated nonframework Al.

3.2. ^{27}Al, ^{29}Si MAS NMR and $^{1}H \rightarrow {}^{29}$Si CP/MAS NMR

Figure 3 displays the ^{27}Al MAS NMR spectra of the zeolites with different crystal sizes. The resonance centered at 56 ppm is commonly assigned to four-coordinated framework aluminum, while the peak at 0 ppm is referred to nonframework octahedral aluminum. As shown in figure 3, the signal for the nonframework aluminum increases with the reduction of the particle size, which reflects a dealumination of the nano-structured HZSM-5 zeolite. Moreover, a distinct broadening of the ^{27}Al (framework) NMR peak with the decrease of the crystal sizes can been observed in figure 3, and the quantitative data showing the change of the width at half height of the peaks have been listed in table 1. According to Casabella, for well-crystallized zeolites the ^{27}Al NMR line width is greatly influenced by the quadrupolar coupling constant (e^2Qq/h) which is due to the local electric field gradients in the sample [15]. The strong surface energy existing on the surface of the small particles will lead to more strain in the lattice, consequently causes the broadening of the main peak of the ^{27}Al MAS NMR line. Similar change of the width of the ^{29}Si MAS NMR lines with crystal size has been identified by inspecting the corresponding ^{29}Si MAS NMR spectra shown in figure 4

Table 1
Properties of various HZSM-5 zeolites measured by XRD, TEM and solid-state NMR.

Sample	Relative crystallinity (%)	Particle size (nm)	Si/Al ratio (NMR)	Concentration of silanols (%)	Line width of ^{29}Si MAS NMR at –114 ppm after deconvolution (Hz)	Line width of ^{27}Al MAS NMR at 56 ppm (Hz)
(a)	73	70	30.7	14	477	940
(b)	79	140	32.2	9	465	868
(c)	100	1000	30.2	4	362	694

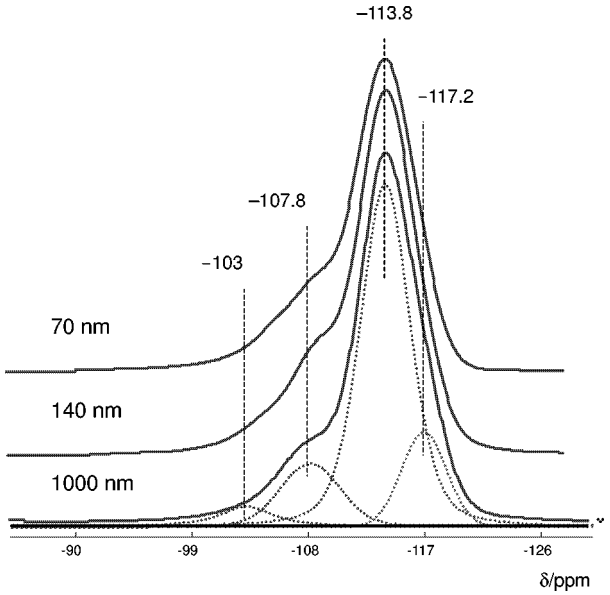

Figure 4. ^{29}Si MAS NMR spectra of HZSM-5 zeolites with different crystal sizes can be deconvoluted using four Gaussian lines.

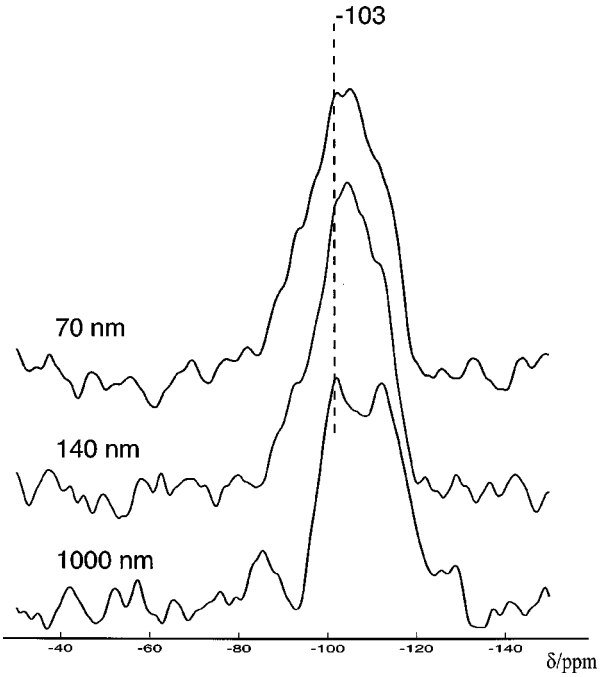

Figure 5. $^{1}H \rightarrow {}^{29}$Si CP/MAS NMR spectra of HZSM-5 zeolites with different crystal sizes. The signal at −103 ppm can be enhanced preferentially under a 1.5 ms contact time for the silicon atoms are connected with hydroxyl groups.

and table 1. A careful deconvolution of the obtained spectra reveals that the apparent broadening of the ^{29}Si MAS NMR line originates dominantly from the expensing of the resonance signal of the Si in SiO_4 tetrahedron surrounded by 4Si with chemical shift at ca. −114 ppm, hence the possible distribution of some amorphous Si to the broadening of the ^{29}Si MAS NMR line could be excluded definitely [16]. It is well understood that lattice strain caused by the decrease in crystal sizes will result in a distribution of the isotropic chemical shift of Si(0Al), which broadens the ^{29}Si MAS NMR line [17]. Analogous changes of the line width were observed by Prasad [18] and Jacobs [19] in their NMR investigations of zeolites with different sizes and have been attributed to the structural alternation of the zeolites.

As demonstrated in figure 4, four peaks in the obtained ^{29}Si MAS NMR spectrum can be well resolved by deconvolution using the Bruker software WINNMR. The peaks at −113.8 and −107.8 ppm are normally assigned to resonances from the Si in the SiO_4 tetrahedra around with 4 and 3 Si atoms, i.e., (4Si, 0Al) and (3Si, 1Al) units, respectively. The shoulder peak centered at about −117.2 ppm was monitored oscillatedly in NMR investigations on aluminosilicate zeolites and was commonly attributed to the existence of crystallographically inequivalent sites in the zeolite [6]. From the Loewenstein's rule [20], the Si/Al ratio for the framework can be calculated from the peak areas in the ^{29}Si MAS NMR spectrum [21]. As shown in table 1, the framework Si/Al ratios of the zeolites with different crystal sizes remain nearly constant at about 30 and no any obvious alternation originated with the change of the synthesis conditions for obtaining zeolites in various crystal sizes.

The peak at −103 ppm in the ^{29}Si MAS NMR spectrum (in figure 4) could be assigned to the silanols, where the terminal hydroxyl groups are connected directly to the Si atom in SiO_4 tetrahedron ($Si(–OH)_1(–OSi)_3$ units). The $Si(OSi)_3OH$ grouping with nonacidic hydroxyl can be facilitated by the use of the $^{1}H \rightarrow {}^{29}$Si cross-polarization technique [7]. As demonstrated in figure 5, the application of CP technique enhances selectively the Si signals (at −103 ppm) of silicon atoms which are coupled with protons of hydroxyl groups by dipolar ^{1}H–^{29}Si interaction. According to the spectra shown in figures 4 and 5, the concentration of the silanol groups increases distinctly with decrease in the zeolite crystal sizes. In HZSM-5 zeolite with a mean size at about 70 nm, the terminal Si such as the SiOH groups is about 14% with respect to the total amount of Si, while only 4% of such silanol groups exists in the same kind of zeolite at 1000 nm crystal size (listed in table 1).

3.3. ^{1}H MAS NMR

High-resolution ^{1}H MAS NMR as a powerful method has been applied frequently to characterize the local environment of protons in zeolites. The different acid sites and acid strengths, as well as their locations in zeolite, can be distinguished by analyzing the chemical shift and shape of the ^{1}H MAS NMR spectra, and by inspecting their changes induced by selective adsorption of the certain molecule probes [22]. Curves (a) and (b) in figure 6 show the ^{1}H MAS NMR spectra recorded from HZSM-5 zeolites with 1000 and 70 nm crystal size, respectively, and the results from quantitative deconvolution of the corresponding spectra are plotted simultaneously. As demonstrated, on the dehydrated HZSM-5 zeolites, five resonance sig-

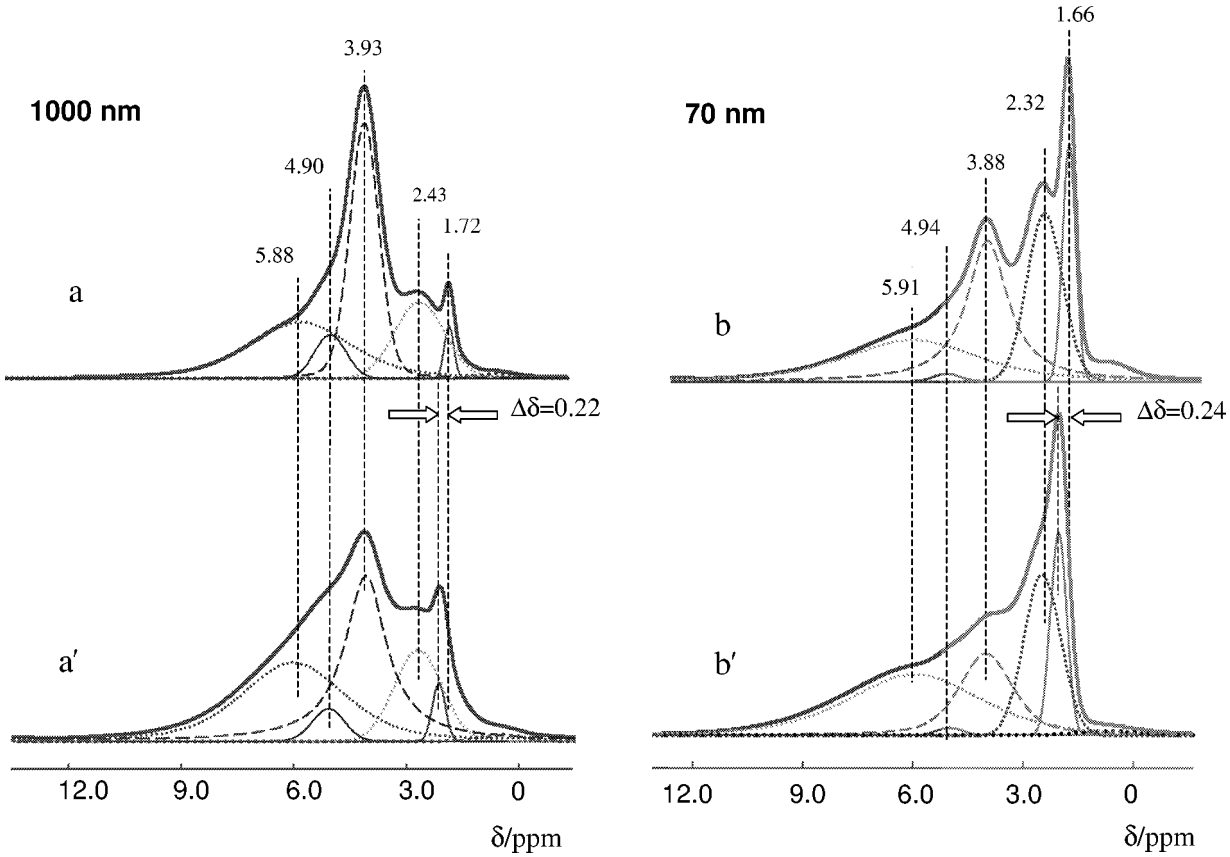

Figure 6. ^{1}H MAS NMR and their deconvoluted spectra of (a, a′) microsized (1000 nm), and (b, b′) nano-structured (70 nm) HZSM-5 zeolites before (top) and after (bottom) adsorption of perfluorotributyl amine.

nals can be identified clearly. The peaks centered at about 1.7 and 3.9 ppm are assigned to the nonacidic hydroxyl groups (silanols) and bridging hydroxyl groups (Si(OH)Al), respectively, while the resonance at about 2.4 ppm is attributed to hydroxyl groups bonded to the extra-framework aluminum [22]. A broad peak centered at about 5.9 ppm can be identified in curves (a) and (b). It is ascribed to a second Brønsted acid site in HZSM-5 zeolites, which have an additional electrostatic interaction with the zeolite framework [22–24]. Figure 6 clearly shows the concentration of silanols is much higher, while that of bridging hydroxyl groups is lower in the HZSM-5 zeolite with 70 nm crystal size. In addition, in this sample, the intensity of the peak at about 4.9 ppm, which is ascribed to the extremely small amount of water molecules adsorbed on Lewis acid sites [25], is much lower, for the nano-structured zeolite with much smaller crystal sizes and shorter channels. The ^{1}H MAS NMR spectra and their deconvoluted spectra after adsorption of perfluorotributyl amine are presented in curves (a′) and (b′) of figure 6. Since perfluorotributyl amine is a weakly basic molecule with a diameter of 0.94 nm [26], which is much larger than the pore size (0.55 nm) of the ZSM-5 zeolite, it should be adsorbed only on the external surface. It can be seen from figure 6 that after adsorption of perfluorotributyl amine, the resonance position of the silanols shifts over 0.24 ppm to the low field. This means that most of the silanols are located on the external surface. For the bridging hydroxyl groups on the external surface, their resonance position after adsorption of perfluorotributyl amine shifts from ∼3.9 to ∼6.0 ppm, which leads to an increase in the integral area of the peak at ∼6.0 ppm. The smaller low-field shift of the silanols ($\Delta\delta_{\mathrm{SiOH}} \approx 0.2$ ppm) induced by the adsorption of perfluorotributyl amine suggests that a weak hydrogen-bond complex is formed due to the relatively high deprotonation energy of the silanols ($\Delta E_{\mathrm{DP}} = 1427\ \mathrm{kJ\,mol^{-1}}$) [24], while for bridging hydroxyl groups on the external surface, the larger low-field shift ($\Delta\delta_{\mathrm{SiOHAl}} \approx 2.0$ ppm) is due to their relatively low deprotonation energy ($\Delta E_{\mathrm{DP}} = 1242\ \mathrm{kJ\,mol^{-1}}$) and the protonation of perfluorotributyl amine to perfluorotributylaminium ions. The low-field shift induced by it is less than that induced by deuterated pyridine due to its much weaker alkalinity [22].

In addition, the bridging hydroxyl groups at the internal surface are not accessible to perfluorotributyl amine, so their chemical shift (at ∼3.9 ppm) will not change. Based on these facts, the concentration of Brønsted acid sites on the external surface can be obtained according to the following equation:

$$C_{\mathrm{ext.surf.}} = (1 - A_1/A_2) \times 100\%, \qquad (1)$$

where A_1 and A_2 denote the integral area of the peak at 3.9 ppm after and before adsorption of perfluorotributyl

amine, respectively, and this integral area can be achieved by deconvolution of the ^{1}H MAS NMR spectra, as shown in figure 6. Based on equation (1), the concentration of Brønsted acid sites on the external surface for nano-structured HZSM-5 zeolites (70 nm) is 35%, while that for microsized HZSM-5 zeolites (1000 nm) is 3%.

4. Conclusions

(1) The line widths of ^{27}Al MAS NMR and ^{29}Si MAS NMR are found to correlate directly to the crystal sizes of zeolites. The smaller the crystal dimension is, the more significant the line broadening of the relating MAS NMR spectrum is.

(2) The proportion of the nonacidic hydroxyl with respect to the total amount of hydroxyl groups in the zeolite increases with the reduction in crystal size. In the HZSM-5 zeolite with an average size of $\sim$70 nm, nonacidic hydroxyls such as SiOH groups are about 14% with respect to the total amount of Si, while only 4% of such hydroxyl groups exists in the same kind of zeolites with 1000 nm crystal size. As evidenced by the selective adsorption of perfluorotributyl amine, most of the nonacidic hydroxyl groups (silanols) are located dominantly on the external surface of the zeolites.

(3) The concentration of the bridged hydroxyl groups (Brønsted acid site) is pronouncedly higher on the surface of nano-structured HZSM-5 than on the surface of the microsized zeolite.

Acknowledgement

We are grateful to the support of National Natural Science Foundation of China and the Ministry of Science and Technology of China through the Climbing Project. We also thank Ms. Xiumei Liu for assistance with NMR experiments and Mr. Dali Tan for TEM measurements.

References

[1] D. Fraenkel, Ind. Eng. Chem. Res. 29 (1990) 1814.
[2] C.R. Kennedy, R.B. LaPierre, C.J. Pereira and R.J. Mikovsky, Ind. Eng. Chem. Res. 30 (1991) 12.
[3] K. Rajagopalan, A.W. Peters and G.C. Edwards, Appl. Catal. 23 (1986) 69.
[4] M.A. Camblor, A. Corma and A. Martinez, Appl. Catal. 55 (1989) 65.
[5] M. Sugimoto, H. Katsuno, K. Takatsu and N. Kawata, Zeolites 7 (1987) 503.
[6] E. Brunner, H. Ernst and D. Freude, J. Catal. 127 (1991) 34.
[7] M. Hunger, J. Karger, H. Pfeifer, J. Caro, B. Zibrowius, M. Buelow and R. Mostowicz, J. Chem. Soc. Faraday Trans. 83 (1987) 3459.
[8] M. Hunger, D. Freude, T. Frohlich, H. Pfeifer and W. Schwieger, Zeolites 7 (1987) 108.
[9] V.P. Shiralkar, P.N. Joshi, M.J. Eapen and B.S. Rao, Zeolites 11 (1991) 511.
[10] E.J. Munson, D.B. Ferguson, A.A. Kheir and J.F. Haw, J. Catal. 136 (1992) 504.
[11] E.J. Munson, D.K. Murray and J.F. Haw, J. Catal. 141 (1993) 733.
[12] T. Xu and J.F. Haw, Topics Catal. 4 (1997) 109.
[13] M. Yamamura, K. Chaki, T. Wakatsuki, H. Okado and K. Fujimoto, Zeolites 14 (1994) 643.
[14] B. Adnadjevic, J. Vukicevic, Z. Filipovic-Rojka and V. Markovic, Zeolites 10 (1990) 699.
[15] P.A. Casabella, J. Chem. Phys. 40 (1964) 149.
[16] K.F.M.G.J. Scholle, W.S. Veeman, P. Frenken and G.P.M. van der Velden, Appl. Catal. 17 (1985) 233.
[17] B.C. Gerstein, J. Non-Cryst. Solids 75 (1985) 423.
[18] J.V. Prasad, K.V. Rao, Y.S. Bhat and A.B. Halgeri, Catal. Lett. 14 (1992) 349.
[19] P.A. Jacobs, M. Tielen, J.B. Nagy, G. Debras, E.G. Derouane and Z. Gabelica, in: *Proc. 6th Int. Conf. on Zeolites*, eds. D. Olson and A. Bision (Butterworths, London, 1984) p. 783.
[20] W. Loewenstein, Am. Mineral. 39 (1954) 92.
[21] C.A. Fyfe, G.C. Gobbi, G.J. Kennedy, J.D. Graham, R.S. Ozubko, W.J. Murphy, A. Bothner-By, J. Dadok and A.S. Che, Zeolites 5 (1985) 179.
[22] M. Hunger, Catal. Rev. Sci. Eng. 39 (1997) 345.
[23] L.W. Beck, J.L. White and J.F. Haw, J. Am. Chem. Soc. 116 (1994) 9657.
[24] E. Brunner, J. Mol. Struct. 355 (1995) 61.
[25] M. Hunger, D. Freude and H. Pfeifer, J. Chem. Soc. Faraday Trans. 87 (1991) 657.
[26] J. Take, H. Yoshioka and M. Misono, in: *Proc. 9th Int. Conf. on Catal.*, eds. M.J. Phillips and M. Ternan (The Chemical Institute of Canada, Ottawa, 1988) p. 372.